PERGAMON

Journal of Atmospheric and Solar-Terrestrial Physics 65 (2003) 871–886

Journal of ATMOSPHERIC AND SOLAR-TERRESTRIAL PHYSICS

www.elsevier.com/locate/jastp

Lognormal form of the ring current energy content

M.W. Liemohn*, J.U. Kozyra

Space Physics Research Laboratory, University of Michigan, 2455 Hayward St., Ann Arbor, MI 48109-2143, USA

Received 9 September 2002; received in revised form 24 February 2003; accepted 13 March 2003

Abstract

It is shown that the stormtime ring current energy content, from kinetic simulations, has a lognormal distribution. This type of functional form naturally arises from the superposition of many processes with a common initiation event but with differing growth and decay timescales. For the ring current, such a situation occurs from the disparate timescales of energization and decay for the hot ions at various energies, pitch angles, and spatial locations. The summation of this plethora of small currents results in a single current system (the ring current, both partial and symmetric) that has a loss time scale that decreases and then increases during every storm. The consequence is that the stormtime D_{st} index, which also has a lognormal shape, can be (and in fact is) dominated by this single current system.

Keywords: D_{st} index; Ring current; Geomagnetic storms; Magnetospheric physics

1. Introduction

A lognormal distribution is a Gaussian "bell" curve where the abscissa values are logarithmic rather than linear,

$$A(x) = \frac{1}{\sigma\sqrt{2\pi}} \exp\left[-\frac{1}{2}\left(\frac{\ln(x)-\mu}{\sigma}\right)^2\right], \quad (1)$$

where μ is a natural logarithm of the value in x where A is a maximum, and σ is a width parameter. Campbell (1996) applied this functional form to the D_{st} index during storm times, concluding that these negative excursions in D_{st} can be well-described by a lognormal distribution. As noted in that study and references therein (e.g., Aitchison and Brown, 1957; Koch and Link, 1980), lognormal distributions are found throughout nature whenever a given signal can be attributed to a collection of smaller signals that have a common trigger mechanism (so they all begin their growth simultaneously) but with a variety of growth and decay timescales.

Because of the goodness of the fits to D_{st}, Campbell (1996) concluded that the stormtime D_{st} signature must also be the summation of the magnetic perturbations from a large number of current systems in the ionosphere-magnetosphere system. In particular, Campbell (1996) claimed the common association of stormtime D_{st} with the amplitude of the symmetric ring current (e.g., Akasofu and Chapman, 1961) was incorrect. The paper went on to describe the various current systems that can also contribute to the stormtime D_{st} signature, with the conclusion that they all must be roughly equal, or at least that D_{st} is not dominated by any single current system.

In their review of geomagnetic storms, Gonzalez et al. (1994) described a few of the well-known contributors to D_{st}, and defined a secondary index D^*_{st},

$$D^*_{st} = \frac{D_{st} - D_{MP} + D_Q}{C_{IC}} \quad (2)$$

as the contribution to D_{st} from near-Earth current systems. In Eq. (2), the terms being removed from D_{st} are the perturbations from the magnetopause Chapman–Ferraro currents $D_{MP} = 15.5\sqrt{P_{sw}}$ (solar wind dynamic pressure in nPa), a quiettime offset $D_Q = -20$ nT, and the influence of induced currents from the diamagnetic Earth $C_{IC} = 1.3$. The subtraction of these terms, however, does not remove the lognormal functional form (as will be discussed below). It would

* Corresponding author. Fax: 734-647-3083.
E-mail address: liemohn@umich.edu (M.W. Liemohn).

1364-6826/03/$ - see front matter
doi:10.1016/S1364-6826(03)00088-9

appear, then, that Campbell (1996) is correct in debunking the dominance of the ring current at producing the stormtime D_{st} index.

A major reason for the long-standing belief in symmetric ring current dominance is from the ability of observed ion distributions to reproduce the stormtime D^*_{st} profile by converting the total ion energy content in the inner magnetosphere E_{RC} to a globally averaged magnetic perturbation. This is commonly done through application of the Dessler–Parker–Sckopke (DPS) equation (Dessler and Parker, 1959; Sckopke, 1966), written for the Earth as

$$D^*_{st_{DPS}}[\mathrm{nT}] = -3.98 \times 10^{-30} E_{RC}[\mathrm{keV}]. \quad (3)$$

This is a robust relation valid for any pitch angle distribution, energy spectra, or spatial distribution of the ion energy. However, there are numerous assumptions built in to this formula, most notably that it was derived for azimuthal currents only. While local time asymmetries in the total ion energy content are handled by Eq. (3) (Carovillano and Maguire, 1968), their field-aligned and ionospheric closure currents are not included in Eq. (3). It is the magnetic perturbations from the network of high-latitude field-aligned currents and ionospheric currents that Campbell (1996) claim are main contributors to the stormtime D_{st}. Despite the implicit assumptions, Eq. (3) has been used successfully to match ion observations to the stormtime D^*_{st} profile (e.g., Hamilton et al., 1988; Roeder et al., 1996; Greenspan and Hamilton, 2000).

More recently, Liemohn et al. (2001a, b) showed that the stormtime ring current is highly asymmetric in the main phase and early recovery phase of magnetic storms. By applying the DPS relation (for the total ion content, including any local time asymmetries, but neglecting perturbations from other near-Earth currents), they reproduced the stormtime D^*_{st} index within some reasonable error for the storms they considered. Other ring current simulations, using the same approach, also successfully reproduce the stormtime D^*_{st} time series (e.g., Jordanova et al., 1998, 1999, 2001; Kozyra et al., 1998, 2002; Ebihara and Ejiri, 1998, 2000). Using the modeled asymmetries, in situ observations can now reproduce the observed D^*_{st} values with even higher accuracy (Greenspan and Hamilton, 2000; Turner et al., 2001).

So, there appears to be a discrepancy. How can the stormtime D^*_{st} signature be a lognormal distribution while at the same time data and theory studies can reproduce the stormtime D^*_{st} index with only the perturbation from the azimuthal component (partial and symmetric) of the ring current? This study addresses this issue by considering the growth and decay timescales of the stormtime ring current from simulations, as well as considering the magnitude of the globally averaged perturbations from a number of other near-Earth current systems. It is concluded that the stormtime ring current is fully capable of producing a lognormal distribution because the loss timescale is dependent on particle species, pitch angle, energy, and spatial location in the inner magnetosphere.

2. Selected storms

2.1. Observations

Six storms were chosen for examination in this study. Their observed D_{st} and D^*_{st} minimum values, along with the times of these minima, are listed in Table 1. They are a diverse group of storms, ranging from moderate size to superstorm class, spanning most of the range of seasonal and solar cycle phases. The one commonality among these storms is that they are all driven by interplanetary coroal mass ejections (ICMEs) and their precursor shocks. They are also chosen for this study because they have been previously simulated by the authors with a kinetic transport code (usually because the event is part of a coordinated campaign investigation). Another selection criterion is that they are all single dip storms, as compared to more complicated double-dip storms (Kamide et al., 1998; Kamide, 2001). While there are only 6 storms being examined, they were not chosen specifically for this study; that is, it is hoped that their unbiased selection provides a degree of generality to the result.

Fig. 1 shows the D_{st} time series for the 6 events. Also shown in each panel are lognormal fits to the data, using the formula

$$D_{st_{LNF}}(t) = D_{off} + \frac{D_{amp}}{\sigma\sqrt{2\pi}} \exp\left[-\frac{1}{2}\left(\frac{\ln(t)-\mu}{\sigma}\right)^2\right]. \quad (4)$$

This equation is very similar to Eq. (1) except for two new factors, D_{off} and D_{amp}. D_{off} is an offset value applied to the entire fit and is set to the average of D_{st} over the first 12 h shown in each panel (that is, the prestorm D_{st} level). D_{amp} is an amplitude factor to scale the lognormal fit to the observed depth of the perturbation. The fits are performed by calculating the error δ between the fitted and the observed values at each abscissa value within a chosen interval,

$$\delta = \sqrt{\frac{1}{N-1}\sum_{t=1}^{N}(D_{st_{LNF}}(t) - D_{st}(t))^2} \quad (5)$$

then randomly changing the fit parameters (D_{amp}, μ, and σ) by up to 1%, recalculating the fit and the error, replacing the saved fit parameters if the error is lower, and continuing this random walk for ten thousand iterations. Several initial guesses are used for each fit to ensure that an absolute minimum is found. Note that Eq. (5) is essentially a standard deviation, except that instead of being the difference from the mean value of the lognormal fits, it is the difference from the observed D_{st} time series. Two fits are shown in each panel of Fig. 1: one over an interval spanning only the peak of the storm (including 6 h before the D_{st} minimum up to 12 h after the minimum), and another over the entire 3 day interval shown in the plot. The best fit parameters and the final error values for these fits are given in Tables 2 and 3.

Table 1
Storm information

Storm	$D_{st_{min}}$	$t(D_{st_{min}})$	$D^*_{st_{min}}$	$t(D^*_{st_{min}})$	$D^*_{st_{DPS,min}}$	$t(D^*_{st_{DPS,min}})$
5/97	−115.0	15.500	−120.0	15.458	−72.0	15.527
9/98	−207.0	25.375	−200.0	25.292	−211.0	25.215
10/98	−112.0	19.625	−126.0	19.167	−107.0	19.208
10/99	−231.0	22.250	−247.0	22.292	−131.0	22.325
4/00	−321.0	7.000	−315.0	7.000	−302.0	7.069
5/00	−147.0	24.333	−169.0	24.167	−158.0	24.166

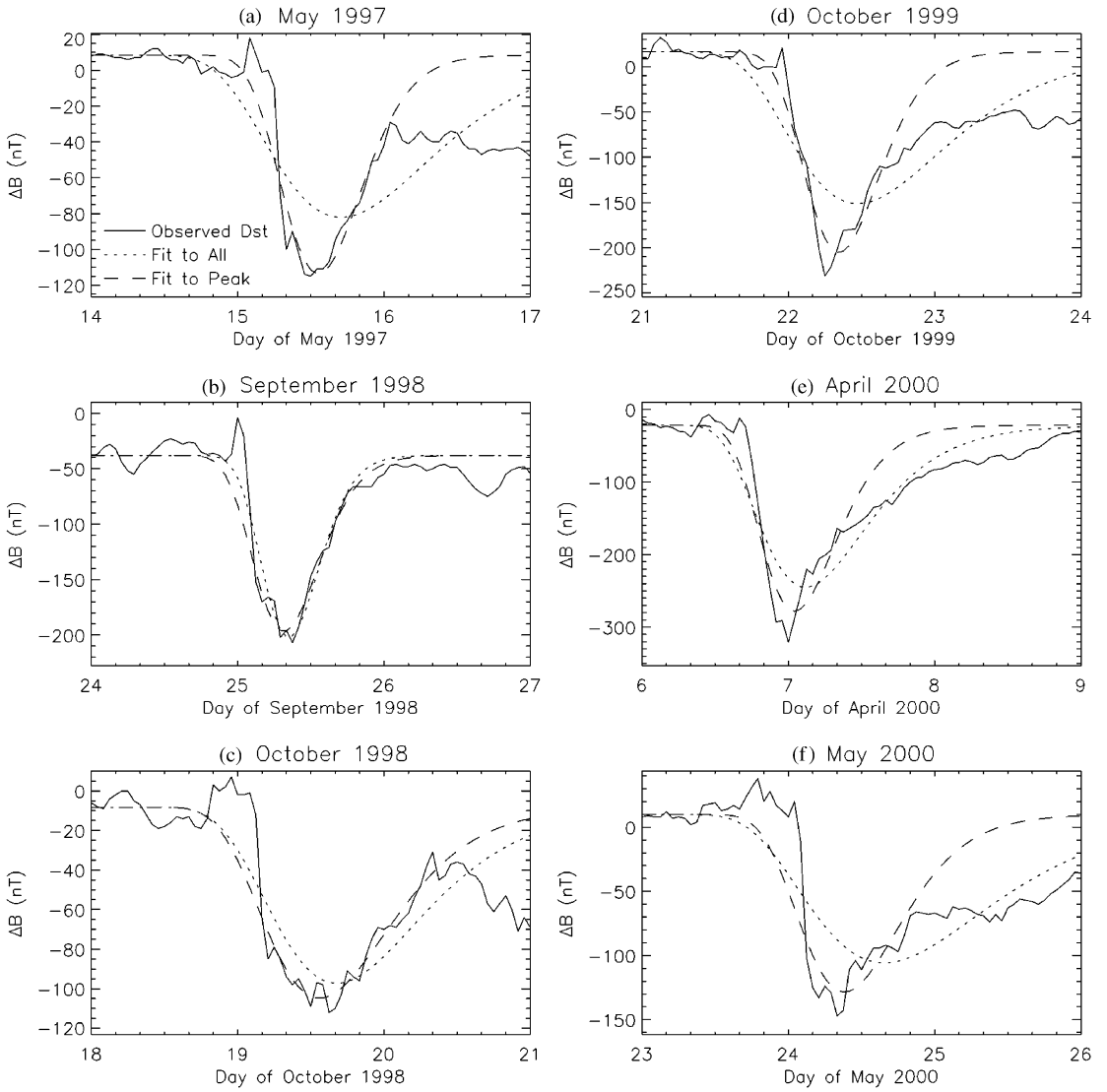

Fig. 1. Observed D_{st} for the 6 storms and lognormal fits.

Table 2
Fits to D_{st}: $(-6,+12)$ h around peak ($D_{st_{min}}$)

Storm	D_{off}	D_{amp}	$t(\mu)$	σ	δ
5/97	8.461	−52.62	15.552	0.1719	12.22
9/98	−38.00	−66.28	25.316	0.1666	9.112
10/98	−8.230	−65.19	19.560	0.2693	5.471
10/99	16.30	−102.8	22.345	0.1851	20.89
4/00	−21.84	−154.2	7.042	0.2402	32.32
5/00	9.769	−83.85	24.382	0.2417	21.44

Table 3
Fits to D_{st}: all 3 days of values

Storm	D_{off}	D_{amp}	$t(\mu)$	σ	δ
5/97	8.462	−71.67	15.707	0.3156	21.59
9/98	−38.00	−58.07	25.349	0.1412	16.82
10/98	−8.231	−66.50	19.677	0.2979	18.13
10/99	16.31	−145.0	22.474	0.3449	33.94
4/00	−21.85	−177.8	7.117	0.3176	31.80
5/00	9.769	−105.0	24.654	0.3626	26.20

Note that, because the stormtime excursion of D_{st} is a negative perturbation, D_{amp} is always negative and D_{off} is usually negative. The errors range from 5 to 34 nT, indicating that the fits are, in general, quite good. It can be concluded, therefore, that the D_{st} time series for these storms are indeed lognormal distributions and, by definition, formed from the superposition of perturbations from many current systems with a range of growth and decay timescales.

Because several of the contributors to D_{st} are well known, it is useful to remove these from the index values, according to Eq. (2), and perform a similar fit and error calculation for D^*_{st}. Fig. 2 shows such fits for the 6 storms. As above, two fits were performed, one over an 18-hour window surrounding the storm peak and another for the entire 3-day interval shown in the panels. The best fit parameters and final errors are listed in Tables 4 and 5 for the two fit intervals, respectively. It is seen that the errors range from 10 to 28 nT, as good, in general, as the lognormal fits to D_{st}. Thus it can be concluded that D^*_{st} is also a lognormal distribution and produced by many current systems.

2.2. Simulation results

Ring current numerical simulations are becoming increasingly adept at reproducing this D^*_{st} time series by applying the DPS relation to the modeled total ion energy content. This study will use such simulation results to produce a synthetic D^*_{st} time series for each storm. The code to be used is that of Liemohn et al. (2001a), which solves the gyration and bounce average kinetic equation for H^+ and O^+ inside of geosynchronous orbit. The energy range of the calculation extends from 10 eV to 400 keV in 42 geometrically spaced steps, covering the entire equatorial pitch angle range with 71 nonuniformly spaced steps (highly resolved near the loss cone boundary), 24 evenly spaced local time steps, and 20 evenly spaced radial distance steps in the equatorial plane. The solution over the roughly 1.5 million phase space grid cells (for each species) is advanced with a time step of 20 s. Second-order accurate numerical techniques are applied to achieve a high-fidelity output from the code. Drift from corotation, convection, and gradient-curvature drift are applied to advect the phase space density through the simulation domain, and various loss processes (Coulomb scattering and decay, precipitation into the atmosphere, and charge exchange) are applied in each grid cell to produce a realistic result. Please see Fok et al. (1993), Jordanova et al. (1996), and Liemohn et al. 1999 Liemohn et al. (2001a) for further details of the numerical scheme and accuracy of the code.

Just as with the observed D_{st} and D^*_{st} values, the modeled D^*_{st} values can be fitted with a lognormal distribution. Fig. 3 shows the modeled D^*_{st} time series for each event, along with the two lognormal fits, as in Figs. 1 and 2. The modeled D^*_{st} minima and the times at which they occur are given in Table 1, and the best fit parameters for the modeled D^*_{st} values are listed in Tables 6 and 7 for the two fit intervals. The errors range from 5 to 27 nT, which is in the same range as the errors for the observed D_{st} and D^*_{st} values for these storms. In fact, considering only the best of the two lognormal fits for each storm, the modeled D^*_{st} values have a lower error for 4 of the 6 storms compared to D_{st} and a lower error for 5 of the 6 storms compared to D^*_{st}. Thus it can be concluded that the modeled D^*_{st} values are

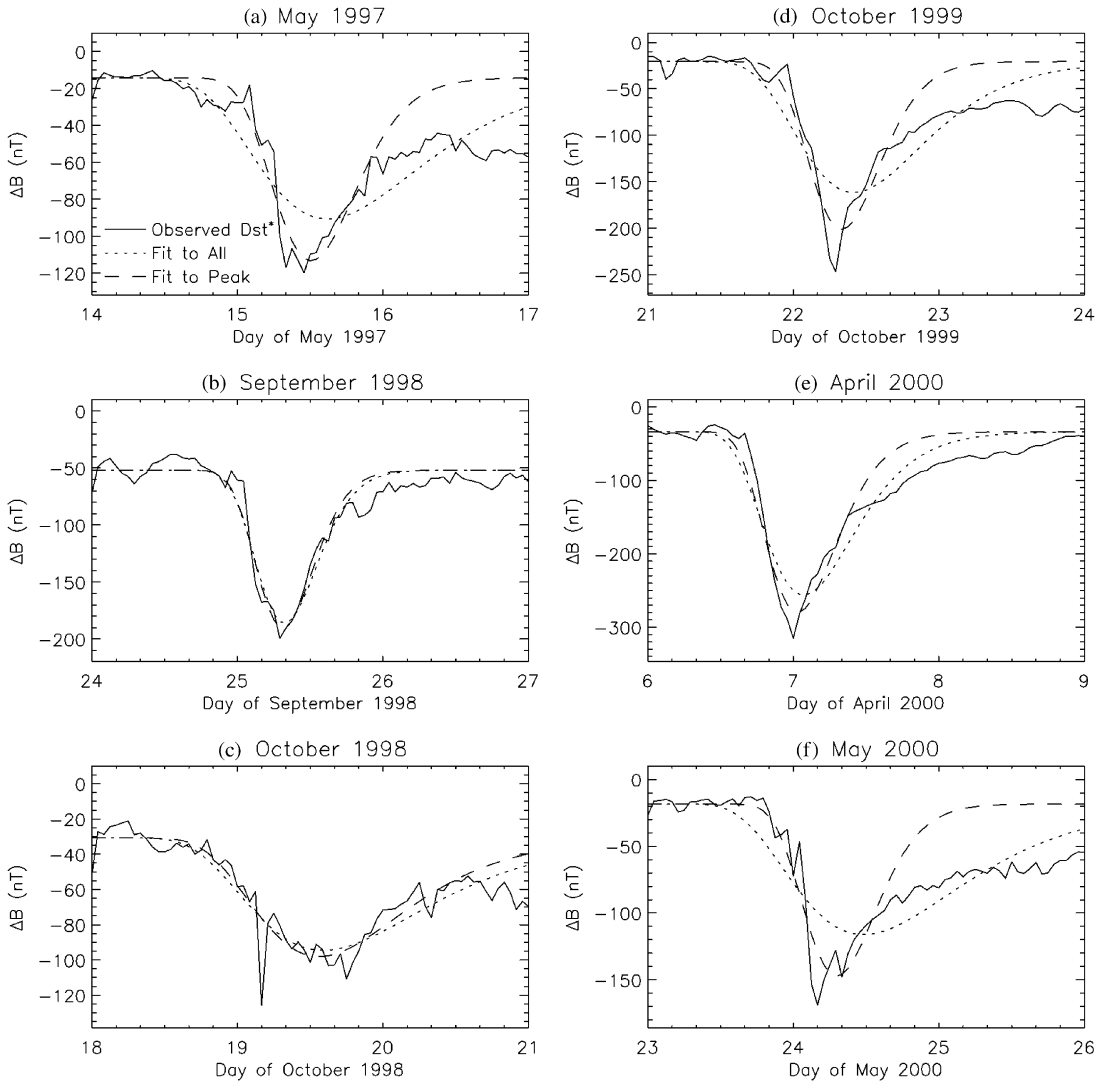

Fig. 2. Observed D^*_{st} for the 6 storms and lognormal fits.

Table 4
Fits to D^*_{st}: $(-6, +12)$ h around peak ($D^*_{st_{min}}$)

Storm	D_{off}	D_{amp}	$t(\mu)$	σ	δ
5/97	−14.30	−45.74	15.506	0.1843	10.49
9/98	−51.88	−50.76	25.313	0.1464	11.78
10/98	−30.77	−53.89	19.561	0.3193	13.02
10/99	−20.56	−80.46	22.332	0.1776	22.63
4/00	−33.68	−139.9	7.029	0.2266	20.97
5/00	−18.40	−60.10	24.298	0.1861	19.17

also lognormal distributions and that they are also created by the summation of perturbations from many small current systems.

There is an obvious question to ask: why is the storm-time ring current behaving like a collection of many small currents? The answer is clear, once the source and losses

Table 5
Fits to D_{st}^{*}: all 3 days of values

Storm	D_{off}	D_{amp}	$t(\mu)$	σ	δ
5/97	−14.30	−64.91	15.618	0.3392	14.99
9/98	−51.88	−52.13	25.324	0.1550	12.06
10/98	−30.77	−59.03	19.589	0.3694	10.58
10/99	−20.56	−104.5	22.414	0.2956	28.10
4/00	−33.68	−155.1	7.0716	0.2780	24.51
5/00	−18.40	−92.79	24.481	0.3788	19.92

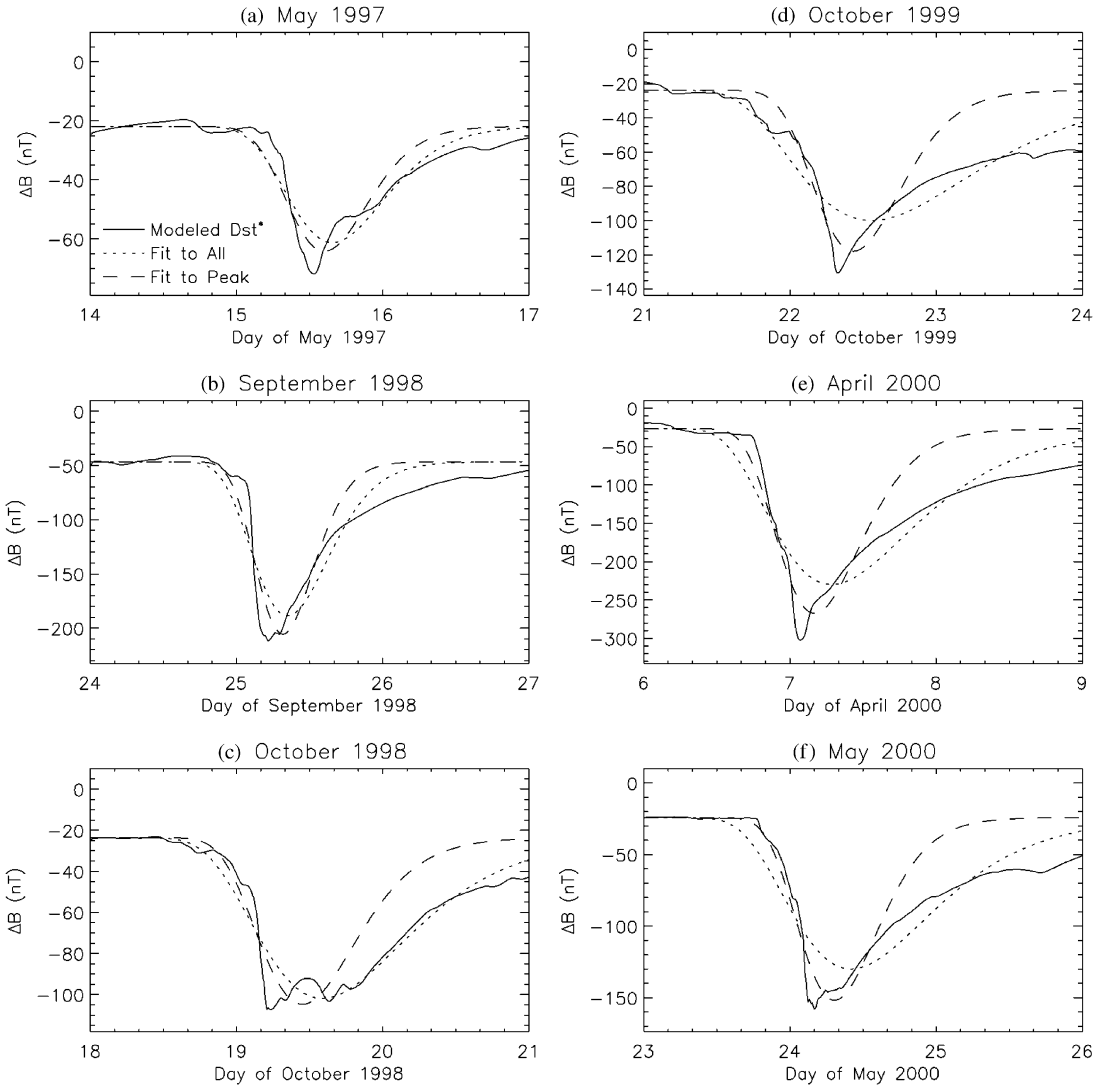

Fig. 3. Modeled D_{st}^{*} for the 6 storms and lognormal fits.

of the stormtime ring current are considered. The stormtime ring current can, in fact, be regarded as a collection of many small currents (arcs as well as rings, for the partial and symmetric components, respectively), that all have simultaneous growth initiation but all have unique growth and decay timescales.

Table 6
Fits to $D^*_{st_{DPS}}$: $(-6, +12)$ h around peak ($D^*_{st_{min}}$)

Storm	D_{off}	D_{amp}	$t(\mu)$	σ	δ
5/97	−21.86	−17.90	15.601	0.1687	6.044
9/98	−46.51	−58.55	25.318	0.1469	20.45
10/98	−23.66	−45.58	19.452	0.2241	10.54
10/99	−24.01	−47.29	22.434	0.2009	7.878
4/00	−26.86	−143.2	7.169	0.2373	20.79
5/00	−24.27	−64.68	24.304	0.2023	10.72

Table 7
Fits to $D^*_{st_{DPS}}$: all 3 days of values

Storm	D_{off}	D_{amp}	$t(\mu)$	σ	δ
5/97	−21.86	−19.36	15.657	0.1961	4.651
9/98	−46.51	−67.02	25.350	0.1881	17.16
10/98	−23.66	−61.45	19.587	0.3134	6.812
10/99	−24.01	−72.79	22.558	0.3824	10.26
4/00	−26.86	−187.0	7.285	0.3676	27.56
5/00	−24.27	−88.19	24.417	0.3329	14.75

3. Discussion of a Lognormal D_{st}

One of the reasons for the continuing misconception of a symmetric stormtime ring current with a single decay constant is the widespread usage of the results of Burton et al. (1975). This study considered solar wind, IMF, and D_{st} data for 10 storms in 1967 and 1968, obtaining a prediction algorithm for D_{st},

$$\frac{d}{dt}D_{st_0} = F - \frac{D_{st_0}}{\tau}, \tag{6}$$

where D_{st_0} is D^*_{st} without the division by C_{IC}. They empirically determined the coefficient values for D_{st_0} (as listed above for Eq. (2)), for the decay constant $\tau = 7.7$ h, and for the growth (actually, D_{st} decrease) factor

$$F = \min[0, -5.4(E_y - 0.5)], \tag{7}$$

where E_y is the GSM-y component of the solar wind motional electric field. Because they condensed the loss rate into a single constant value, and this prediction formula works with some reasonable degree of accuracy (e.g., Lindsay et al., 1999), the misconception gained credence.

Recently, however, a reanalysis of the terms in Eq. (6) has been performed (O'Brien and McPherron, 2000a). While most of the coefficients remained similar to the Burton et al. (1975) values, they recognized that the recovery timescale of D_{st_0}, like its growth term, also systematically varies with E_y. By considering that the Alfvén boundary moves as a function of magnetospheric convection strength, which varies as a function of E_y, they found a physical reason for choosing an exponential function form, and then fit the coefficients to obtain the following equation for τ,

$$\tau[\text{h}] = 2.40 \exp\left[\frac{9.74}{4.69 + \max(0, E_y)}\right] \tag{8}$$

which yields $\tau = 19.1$ h for $E_y \leqslant 0$ and then decreases with increasing E_y. From Eq. (8), τ passes through the 7.7 h level for $E_y = 3.67$ mV/m. This prediction algorithm works much better than the Burton et al. (1975) formulation (O'Brien and McPherron, 2000b). More complicated D_{st} prediction algorithms (e.g., Temerin and Li, 2002) also use multiple and/or varying decay timescales for the relaxation of the stormtime D_{st} perturbation.

Because D_{st} and D^*_{st} (which is essentially the same as D_{st_0}) exhibit lognormal distributions, it is not surprising that the best prediction algorithms have varying decay timescales. In a magnetic storm, E_y often increases during the main phase and drops during the recovery phase (this is why the prediction algorithms work so well), and therefore τ will change throughout a storm epoch. The basic variation of τ is to drop from a high prestorm value to a minimum value near the time of the D_{st} minimum and then rise back up during the recovery phase. This variation in the decay timescale of D_{st} is an essential element in producing its lognormal shape. That is, considering the concept of many small current systems contributing to D_{st}, the recovery phase rise in τ reflects the transition from dominance by currents that die off rapidly to dominance by those that die off slowly. Thus, a time series of numbers will have a lognormal distribution (at least after the peak value) when the overall decay timescale increases with time after the peak.

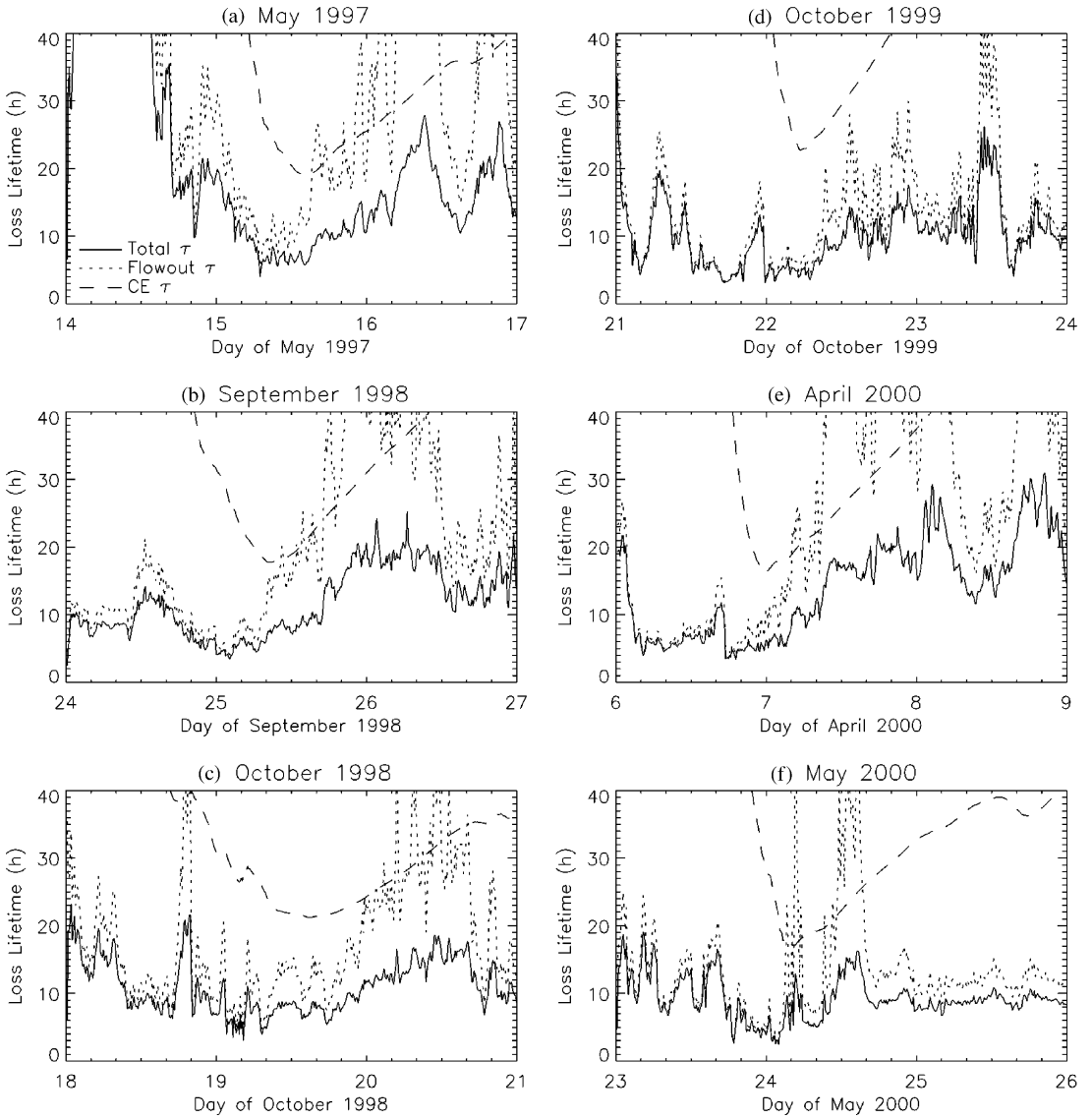

Fig. 4. Modeled ring current energy loss lifetime for all loss processes (solid line), flowout losses only (dotted line) and charge exchange losses only (dashed line).

Let us consider this theory with respect to the ring current simulation results. Accounting of the energy sources Q and losses L can be tallied in the simulation, so a differential equation can be written for the modeled D^*_{st},

$$\frac{d}{dt}D^*_{st_{DPS}} = Q - L \tag{9}$$

and, by analogy to Eq. (6), a total decay timescale can be computed

$$\tau = \frac{D^*_{st_{DPS}}}{L}. \tag{10}$$

This τ would be the exponential decay timescale of $D^*_{st_{DPS}}$ assuming $Q = 0$ (no new input). In addition, a partial loss lifetime τ_i for a specific physical process "i" can be computed from Eq. (10), simply by replacing L with the loss rate for that process alone L_i. These partial loss lifetimes are related to the total loss lifetime by the following formula,

$$\frac{1}{\tau} = \sum_i \frac{1}{\tau_i}, \tag{11}$$

where the summation runs over all of the individual processes. Fig. 4 shows the total loss lifetime from the ring current simulation results as well as the partial loss

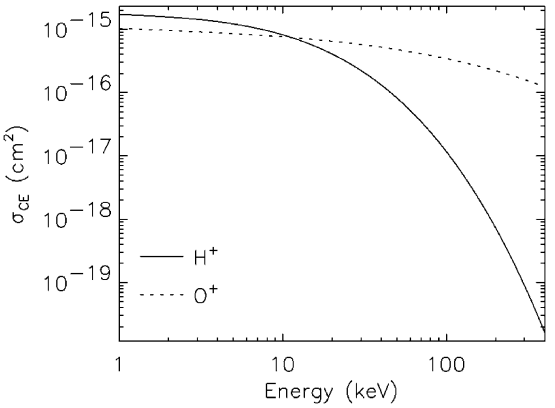

Fig. 5. Charge exchange cross section for H^+ and O^+ (with neutral hydrogen) as a function of energy.

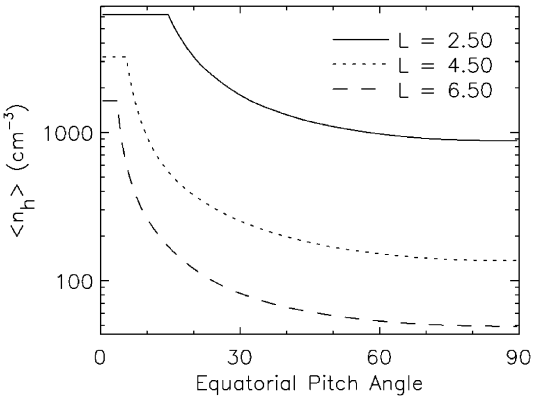

Fig. 6. Bounce-averaged neutral hydrogen geocoronal densities as a function of equatorial pitch angle for three L shells.

lifetimes from the two largest loss mechanisms of the stormtime ring current, flowout through the dayside magnetopause and charge exchange with the neutral hydrogen geocorona. Fig. 4 shows the ever-changing timescale of ring current decay, especially an increasing trend during the recovery phase of the storms, consistent with the hypothesis for the formation of a lognormal distribution.

The cause of this continual variation in τ is also revealed in Fig. 4, which shows the sporadic nature of the flowout loss and the gradual variation of the charge exchange loss. While both lifetimes drop considerably during ring current growth, as expected (Liemohn et al., 1999; O'Brien and McPherron, 2000a), Fig. 4 shows that flowout is responsible for the fastest loss timescales. In fact, the charge exchange timescale never drops below 10 h during these 6 storms. It is interesting to note that for many of the storms, flowout losses sometimes return to shorter timescales late in the recovery phase (and also sometimes in the prestorm epoch). This is not necessarily due to a strong enhancement in the convection (although it certainly could be), but it can result from the total energy content dropping to a point where the mild convective flow of plasma sheet ions through the outer regions of the simulation domain has a bigger loss rate than the charge exchange losses of the decaying symmetric ring current left over from the storm. These flowout losses are matched by nearly equal energy inputs, and so they often do not result in a significant change in modeled D_{st}^*.

The changing partial loss lifetime for charge exchange can be explained by considering the terms that contribute to the charge exchange loss rate. This process can be written as a simple exponential attenuation factor on the phase space density,

$$f_{t+dt} = f_t \exp(-v\Delta t \sigma_{CE} \langle n_H \rangle), \quad (12)$$

which is the calculational method used in the simulations. The first two terms in the exponent of Eq. (12) are simply the velocity of the hot particle (dependent on the energy of the phase space grid cell) and the simulation time step. The third term is the cross section between the hot ion and the cold neutral. Fig. 5 shows σ_{CE} for H^+ and O^+, as a function of energy (technically this should be relative velocity, but it is assumed that the neutral hydrogen atom is always moving very slowly compared to the ion). It is seen that σ_{CE} is highly dependent on both energy and ion species. The fourth term in the exponent of Eq. (12) is the bounce-averaged neutral hydrogen density. In the simulations, the radial distribution of Rairden et al. (1986) is used for the geocorona, with the assumption of spherical symmetry. Integrations for three L values are shown in Fig. 6, as a function of equatorial pitch angle (which determines the mirror-point altitude). Note that the loss cone pitch angles are set to the loss cone boundary value, where it is assumed that all of the particles are lost to the atmosphere with an attenuation factor of half a bounce period. It is seen that $\langle n_H \rangle$ is highly dependent on both L shell and equatorial pitch angle. Therefore even if the stormtime ring current were completely symmetric at all times (which is most likely not the case (e.g., Liemohn et al., 2001a)), the decay timescale would decrease during the growth phase as new plasma is brought into the phase space regions with short lifetimes, and would increase throughout the recovery phase of the storm as these fast lifetime regions were preferentially evacuated.

The other main loss process of the stormtime ring current is flowout (e.g., Takahashi et al., 1990; Liemohn et al., 1999). During periods of low convection electric field, the motion of hot ions in the inner magnetosphere is dominated by gradient-curvature drift, and the particle trajectories are simply westward-flowing circles around the Earth. For strong convection, however, this assumption about the trajectories breaks down. Fig. 7 shows ion drift paths through the inner magnetosphere for 3 magnetic moments (defined as an energy at geosynchronous orbit, $L = 6.6$) in the 3 rows and for 3 convection strengths in the 3 columns (equatorial pitch angle is set to 90° in these plots). The convection electric field description used for these plots is the E5D

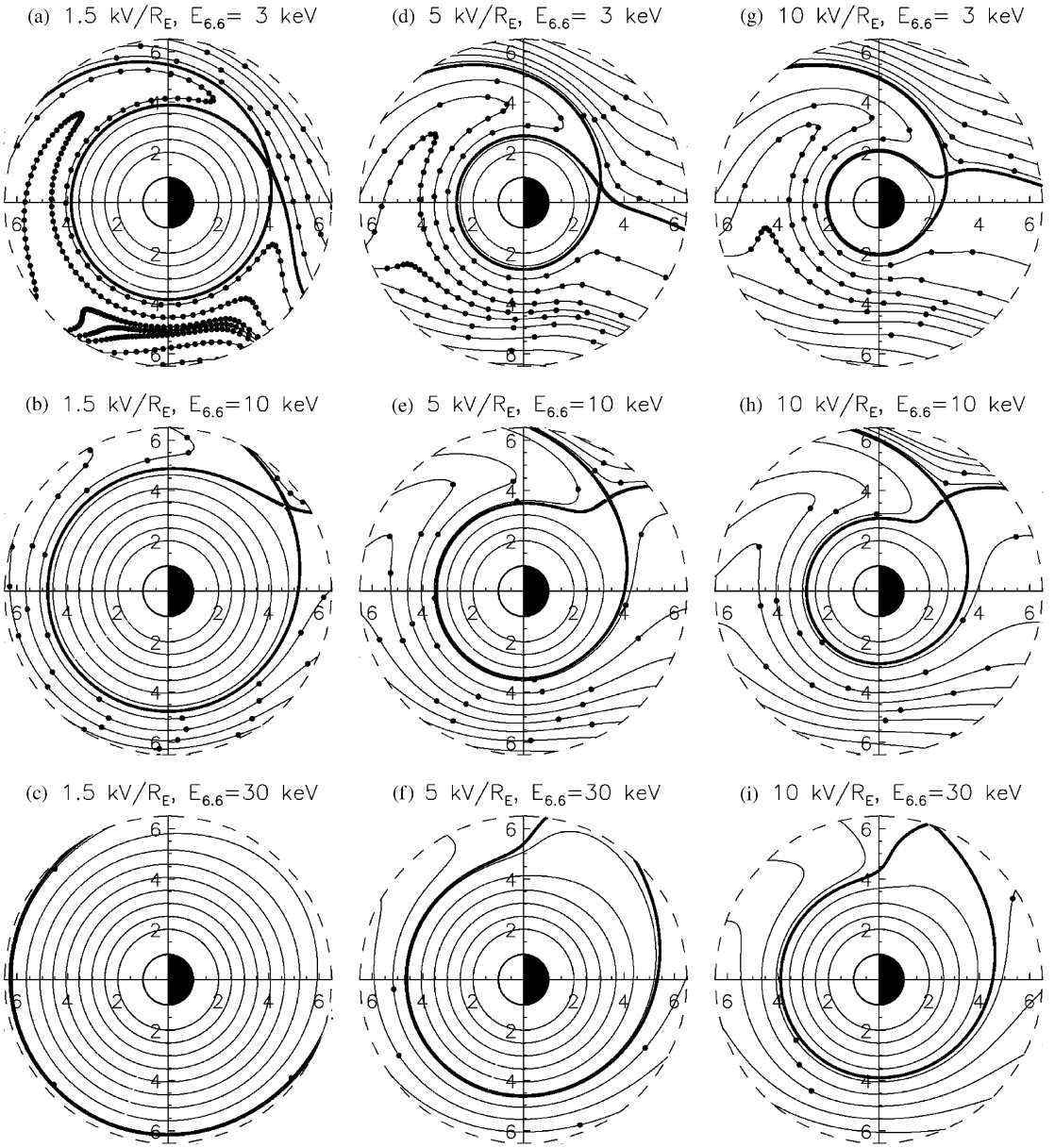

Fig. 7. Ion trajectories for three magnetic moment values and three activity levels.

model of McIlwain (1986), modified to use a cross polar cap potential as a strength parameter instead of Kp (Liemohn et al., 2001a). Black dots are drawn on the open trajectories to demark 1-h drift intervals. The 3 magnetic moments are chosen as low, medium, and high energy values of the typical particle distribution at geosynchronous orbit, and the convection strengths are also chosen to be a low, medium, and high value for the near-Earth cross tail electric field. Flowout from the inner magnetosphere to the dayside magnetopause is highly dependent on the location in phase space (energy, L shell, local time, and equatorial pitch angle). The flight time could range from an hour to several days. The convection strength, however, is also a big factor in determining the rate of flowout. The variations of the partial loss lifetime for flowout seen in Fig. 4 are functions of the time history of the inflow from the plasma sheet, the loss processes acting on the particles inside of the simulation domain (like charge exchange), and the present convection strength. The net result is a complicated time series that wildly jumps throughout the 3-day interval shown for each storm, but in

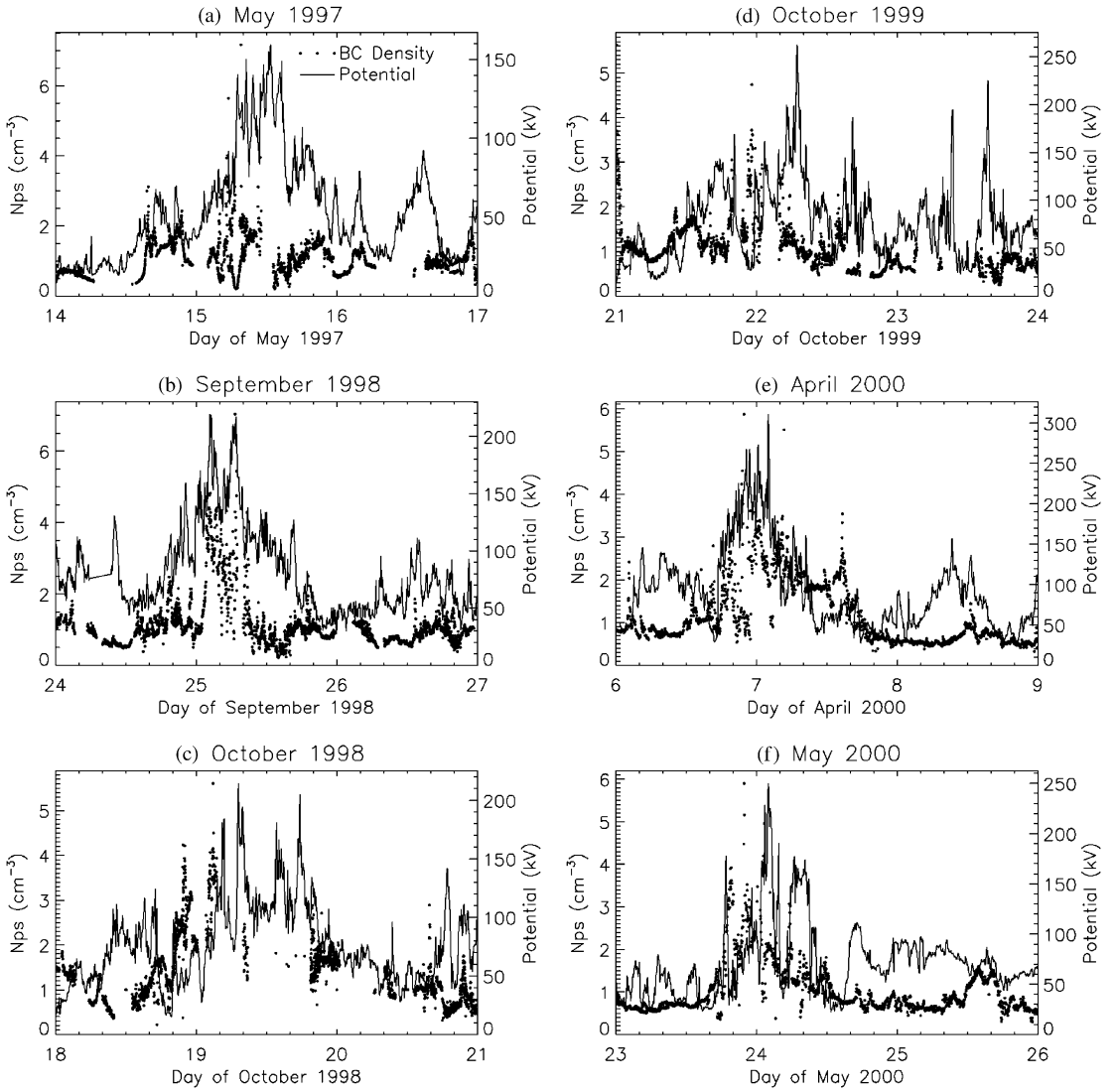

Fig. 8. Nightside plasma sheet density (observed at geosynchronous orbit) and AMIE-derived cross polar cap potential, the two main functions that contribute to the ring current source rate.

general the flowout loss timescale decreases during the main phase and increases during the recovery phase, contributing to the lognormal distribution of the modeled D_{st}^{*} values.

Similarly, the growth rates of these small currents are quite disparate. The stormtime ring current is primarily created through the simultaneous occurrence of high cross polar cap potential and high plasma sheet density. The former causes the majority of phase space in the inner magnetosphere to be part of an open drift path. That is, most of the preexisting hot plasma near the Earth is swept out toward the dayside magnetopause while the near-Earth plasma sheet is swept in to replace it. If the plasma sheet density is elevated (perhaps to a superdense plasma sheet level (Borovsky et al., 1997; Kozyra et al., 1998)), then the ring current will most likely be enhanced. Figure 8 shows these two parameters for the selected events. The nightside near-Earth plasma sheet densities are taken from the magnetospheric plasma analyzers onboard the Los Alamos National Laboratory geosynchronous satellites (Bame et al., 1993). The cross polar cap potentials are found from the results of the assimilative mapping of ionospheric electrodynamics (AMIE) technique (Richmond and Kamide, 1988), using all available magnetometer data. These are the boundary conditions used in the simulations discussed above. By comparing the modeled D_{st}^{*} time series in Fig. 3 with the values shown in Fig. 8, it is seen that the stormtime ring current total

energy content only increases when both of these source functions are elevated. There are numerous intervals during these storms when one of the driver terms is big and the other is small, and consequently there is little total energy increase (in fact, perhaps a decrease, when the potential is high and the density is low, such as near 1200 UT on September 25, 1998). In addition, the injected particles gain (lose) energy as they convect inward (outward) in L shell inside the simulation domain. This adiabatic energization can be dominant at times, especially during the main phase of a storm, but in general the net influence is rather small (e.g., Liemohn et al., 2002). Fig. 7 illustrates the variability of this adiabatic energization as a function of ion magnetic moment and convection strength, as well as the time required to inject particles of a certain energy into a given region of the inner magnetosphere.

This discussion is consistent with the findings of Campbell (1996), who determined that the stormtime D_{st} perturbation has a lognormal distribution. Because of the assumption by Campbell (1996) that the ring current has a single (and constant) decay timescale after a rapid intensification phase, it was argued that the ring current perturbation must be only a small fraction of the D_{st} index. The discussion above shows that the lognormal pattern of D_{st} can in fact be consistent with the idea of D_{st} being primarily a measure of ring current strength.

It should be noted that there is a recent study by Dasso et al. (2002) that fit the stormtime recovery of D_{st} with an exponential decay function. Such a choice requires a single decay constant throughout an event. In their examination of the $\sim$300 storms over the last $\sim$30 years, they found only $\sim$ 25% of the storm recovery phases (the first 12 h after $D_{st_{min}}$) are well fit by this functional form. This indicates that a lognormal fit (increasing τ during recovery) is perhaps a more correct functional form of the stormtime D_{st} index. Close examination of Fig. 4, however, reveals that the total decay timescale can sometimes have a rather flat profile for intervals of several hours, giving theoretical support to the findings of Dasso et al. (2002).

4. Other D_{st} contributors

While the expectation is that the ring current contribution (partial and symmetric) is the main contributor to the stormtime D_{st} perturbation, other current systems influence the index as well. In their study empirical testing the DPS relation, Greenspan and Hamilton (2000) discuss many of the contributors to D_{st}. The reader is referred to that study for a thorough review of this subject, and only a brief synopsis with reference to some additional work is given here. To summarize their findings, they concluded that the DPS relation, using in situ ion flux measurements, is very good at predicting the stormtime D_{st} when the observations are made on the nightside. However, a DPS relation conversion of dayside measurements falls short of the observed D_{st} value. They speculated this was because of the asymmetry of the stormtime ring current, which has now been shown theoretically (e.g., Liemohn et al., 2001a, b) as well as observationally with global energetic neutral atom snapshots of the inner magnetosphere (e.g., Mitchell et al., 2001; Pollock et al., 2001). They concluded that the effects of other current systems on D_{st} are either small or collectively sum up to zero.

There is one current system, the substorm growth phase tail current and subsequent substorm expansion phase current wedge, that has received much attention over the years, and it is useful to examine this one in closer detail. A useful tool in analyzing the midlatitude magnetic signature of substorms is to synthesize data from numerous stations into a local time-universal time (LT-UT) perturbation map. Clauer and McPherron (1974, 1980) analyzed the local time distribution of substorm magnetic perturbations as observed by midlatitude ground-based magnetometers. It was shown that only large substorms could be seen in these data, and they had the standard positive perturbation near midnight (from the current wedge) and a negative perturbation near dusk (from the westward-drifting hot plasma). The timescale of these perturbations was typically around half an hour. These studies focused on isolated substorm signatures, but a similar examination of stormtime substorms revealed a consistent perturbation (Clauer et al., 2003). While the influence on the longitudinal asymmetry is large, the contribution to the globally-averaged perturbation is small (see also the review by Fukushima and Kamide (1973) for early analysis of this problem).

Those studies, however, use $\sim$25 magnetometers to create the LT-UT perturbation maps. Far fewer measurements are used to compute D_{st}, and therefore the position of these stations with respect to the substorm features can lead to a significant influence on the index. Theoretically, Friedrich et al. (1999) found that the substorm current wedge could cause a momentary upswing of up to 45 nT in the perturbation recorded at a station directly equatorward of the wedge. Observationally, Munsami (2000) showed that there is a significant temporary increase in D_{st} when a station lies beneath the wedge (otherwise there was no correlation). The wedge current, however, is shortlived, typically lasting less than an hour.

Shen et al. (2002) have derived a new D_{st} prediction algorithm based on upstream solar wind conditions and the AL index. They find that the "growth" rate of D_{st} (F in Eqs. (6) and (7) above) is dependent on AL, with a different functional form above and below a threshold value of AL = $-$500 nT. A correlation between D_{st} and AL has been shown before (Davis and Parthasarathy, 1967; Cade et al., 1995), so the creation of this form of predictive algorithm is not surprising.

The influence of substorms on the D_{st} index has also been discussed recently in terms of the tail current growth and decay. Rostoker (2000) made the claim that, because Kp and D_{st} are closely related, substorms must play a large

part in the D_{st} signature. This conclusion is based on the assumption that Kp is a measure of substorm activity, and he argues that Kp is a better index for this purpose than AE or AL. Kp is a range index compiled from the Ks indices from about a dozen stations in the upper-midlatitude region (50–65° geomagnetic) (Rostoker, 1972). The Ks index for any given station is found by taking the maximal change for any one component (H: north–south, D: east–west, or Z: up–down) and applying this to one of the lookup tables for that station (dependent on season, latitude, UT, and instrumental effects). Thus, Kp is highly dependent on universal time (i.e., which station is where in LT), the location of the auroral oval, the presence of a strong symmetric or asymmetric ring current, as well as the presence of any substorms within the 3 h cadence of the index. The relationship between Kp and substorms can be summarized like this, "Kp is not a good quantitative indicator of the intensity of a given substorm or level of substorm activity" (Rostoker, 1972, p. 944). So, it is surprising that Rostoker (2000) would use Kp for substorm activity.

What Kp seems quite good at is characterizing the overall level of convection in the magnetosphere. Numerous studies have shown good correlation between Kp and convective strength, from plasmaspheric studies in the early 1970s (e.g., Chappell, 1972, 1974; Grebowsky et al., 1974; Maynard and Chen, 1975) to more recent studies of hot ion plasma flow in the inner magnetosphere (e.g., Fok et al., 1993; Jordanova et al., 1996; Korth et al., 1999; Friedel et al., 2001).

More quantitative approaches to understanding the influence of the tail current include the efforts of Alexeev et al. (1996), Turner et al. (2000, 2001), Feldstein et al. (2000), and Ganushkina et al. (2002). The magnetotail currents in the Alexeev et al. (1996) model can impinge on the inner magnetosphere down to geocentric distances of 3.5 R_E, causing up to 50% of the total simulated D_{st} perturbation. This distance is approaching the observed inner edge of the ring current region (e.g., Frank, 1970; Lui et al., 1987; Roeder et al., 1996). None of the perpendicular current, however, was allowed to close through the ionosphere, but rather continued out to the magnetopause and closed there. This is contrary to the recent observational evidence of midlatitude field-aligned currents (Waters et al., 2001; Clauer et al., 2003) and modeling results that show the stormtime partial ring current can cause such currents (Liemohn et al., 2001b).

Turner et al. (2000) had a different approach, using the T-96 magnetic field model (Tsyganenko and Stern, 1996) to define the stormtime magnetotail current sheet. They found that the tail current can contribute up to −25 nT to the D_{st} index, particularly strong at substorm onset. Their follow-up study (Turner et al., 2001) used a flat rate of 25% for the tail current contribution to the D_{st} index. That number, however, is based on the assumption of 10 major substorms per storm. So 25% is probably too high of a percentage for the influence of the stormtime tail current on D_{st}. Exception has been taken to the Turner et al. (2000) study because of their choice of an $x_{GSM} = -6\ R_E$ cutoff for the tail current calculational box (Maltsev and Ostapenko, 2002; Turner et al., 2002). In their reanalysis, though, Maltsev and Ostapenko (2002), like Alexeev et al. (1996), close all of the longitudinally asymmetric current in the inner magnetosphere through the magnetopause rather than allowing for the existence of a partial ring current that closes through the ionosphere. As Turner et al. (2002) note, the difference between tail current and partial ring current is largely semantical, as they both are carried by particles on open drift paths.

The study by Feldstein et al. (2000) argues that the tail current is also rapidly diminishing during the recovery phase of storms, and that the recovery of the D_{st} index is caused by this decrease. This conclusion is based on results from the Alexeev et al. (1996) model, so again the issue is semantical: the current resulting from particles flowing through near-Earth space (that is, on open drift paths) can be thought of as either tail current or partial ring current, because the two currents smoothly blend into each other. They take issue with the use of the DPS relation for ion energy content on open drift paths, stating that Eq. (3) was originally derived for a symmetric ring of particles in the inner magnetosphere. Maguire and Carovillano (1968), however, showed that the DPS relation works for any spatial distribution, but only takes into account the magnetospheric azimuthal current portions of the circuit. Therefore, the DPS relation is complete for a symmetric ring current, but it is also correct (just incomplete) for a partial ring current. More recently, Liemohn (2003) has shown this applicability extension through numerical calculations. Liemohn (2003) also demonstrated that the DPS relation overestimates the magnetic perturbation from the energy content in the integration volume if the pressure does not go to zero at the volume boundaries. This means that when the plasma pressure in the near-Earth tail is large, a significant portion of the magnetic perturbation as calculated by the DPS relation is actually from the tail current. Such a result might bring resolution to the partial ring current-tail current debate.

In a novel data assimilation approach, Ganushkina et al. (2002) have deconvolved the stormtime inner magnetospheric magnetic field to its source term components by fitting observed field values to a modified T-96 field, where the coefficients of the various current systems were adjusted to match the measurements. They determined that the ring current accounts for most (∼75%) of the stormtime D_{st} perturbation during strong storms ($D_{st_{min}} < -100$ nT), but that the tail current can dominate during smaller D_{st} disturbances. Note, however, that again there is no asymmetric ring current included in the technique, and so the contribution from this dominant current system has been split between the symmetric ring current and tail current contributions in the analysis. Continued analysis with this technique, using the new T-02 model (Tsyganenko, 2000a, b) that includes a partial ring current term, might reveal the true apportionment of the asymmetric currents in the inner magnetosphere.

Ohtani et al. (2001) approached the issue observationally, showing a correlation between geosynchronous dipolarizations (near midnight) and D_{st} recovery. They concluded that the same effect (tail current decrease, coincident with substorm expansion) is the cause of these signatures. The average change in D_{st} was roughly 20 nT while the change at geosynchronous was about 40 nT. The hypothesis, very similar to the Feldstein et al. (2000) result, is plausible, but the relative magnitudes of the perturbation should be much more disparate for a near-Earth tail disruption as the source of the D_{st} recovery. That is, another coincidental factor must be causing the simultaneous D_{st} recovery. This is because the Biot–Savart law scales the magnetic perturbation strength with distance from the current as $1/r^2$. Therefore, the disruption in the tail current must be very strong and quite far from geosynchronous orbit to solely account for both signatures.

From the above discussion, it is clear that there is evidence for a substorm contribution to the D_{st} index. However, as concluded by Greenspan and Hamilton (2000), the influence is most likely short-lived (an hour or less) and canceled out in the global averaging (e.g., the oppositely directed current wedge and hot ion drift perturbations). It should be noted that several recent reviews of the ring current's connection to geomagnetic storms exist, including Gonzalez et al. (1994), Daglis (2001), and Kamide (2001), all of which contain discussions of the storm-substorm relationship but pose it as an open issue still waiting for a conclusive answer.

5. Conclusions

It has been shown that the total energy content of the stormtime ring current has a lognormal distribution because of the phase-space-dependent (and species-dependent) decay timescale for hot ions in the inner magnetosphere. The ring current has an ever-changing growth and decay timescale because it is the net effect of hot ions at many energies, pitch angles, and spatial locations. Therefore it is possible for the ring current to be the major contributor to the D_{st} index, which also has a lognormal distribution. Of course, other current systems contribute to D_{st}, but their influence is most likely minor during storm events.

As models and data products improve, the issue of what contributes to the stormtime D_{st} signature can be more definitively answered. This is not a refutation of the findings of Campbell (1996), therefore, but rather a continuation of that work. He concluded that the D_{st} index is formed by the summation of perturbations from many small current systems. The same conclusion is drawn here. The difference is in the identification of the "many small currents." In this study, they are primarily the circles and arcs through hot ion phase space in the inner magnetosphere. The contrast between the current identification of Campbell (1996) and this study arises for three main reasons. First, the stormtime ring current is not assumed to be symmetric during storms, but rather is believed to be asymmetric for most of the storm epoch. Second, the stormtime ring current (symmetric or asymmetric) can be thought of as many small currents, each with its own growth and decay timescale, rather than having a single, constant timescale throughout each storm event. Third, new analyses have shown that the DPS relation works well for converting the total inner magnetospheric ion energy content value to D_{st} and vice versa. The end result is that the lognormal pattern of D_{st} is consistent with the idea of D_{st} being primarily a measure of ring current strength.

Acknowledgements

This study was supported by the National Science Foundation under grant ATM-0090165 and by the National Aeronautics and Space Administration under grants NAG5-10297 and NAG-10850. The authors would like to thank all of their data providers who made the ring current simulations possible, especially M.F. Thomsen, J.E. Borovsky, and G.D. Reeves at the Los Alamos National Laboratory, F. Rich at the Air Force Research Laboratory in Hanscom, MA, A.J. Ridley and G. Lu for the supplying the cross polar cap potentials used in these simulation runs, the Kyoto World Data Center for the D_{st} index, and CDAWeb for allowing access to the plasma and magnetic field data of the Wind and ACE spacecraft.

References

Aitchison, J., Brown, J.A.C., 1957. The Lognormal Distribution With Special Reference to its Use in Economics. Cambridge University Press, Cambridge.

Akasofu, S.I., Chapman, S., 1961. The ring current, geomagnetic disturbance and the Van Allen radiation belts. Journal of Geophysical Research 66, 1321.

Alexeev, I.I., Belenkaya, E.S., Kalegaev, V.V., Feldstein, Y.I., Grafe, A., 1996. Magnetic storms and magnetotail currents. Journal of Geophysical Research 101, 7737–7747.

Bame, S.J., et al., 1993. Magnetospheric plasma analyzer for spacecraft with constrained resources. Review of Science Instruments 64, 1026.

Borovsky, J.E., Thomsen, M.F., McComas, D.J., 1997. The superdense plasma sheet: plasmaspheric origin, solar wind origin, or ionospheric origin? Journal of Geophysical Research 102, 22089.

Burton, R.K., McPherron, R.L., Russell, C.T., 1975. An empirical relationship between interplanetary conditions and D_{st}. Journal of Geophysical Research 80, 4204–4214.

Cade, W.B.III, Sojka, J.J., Zhu, L., 1995. A correlative comparison of the ring current and auroral electrojets using geomagnetic indices. Journal of Geophysical Research 100, 97.

Campbell, W.H., 1996. Geomagnetic storms, the D_{st} ring-current myth and lognormal distributions. Journal of Atmospheric and Terrestrial Physics 58, 1171.

Carovillano, R.L., Maguire, J.J., 1968. Magnetic energy relationships in the magnetosphere. In: Carovillano, R.L.,

McClay, J.F., Radoski, H.R. (Eds.), Physics of the Magnetosphere. Reidel, Norwell, MA, pp. 290.

Chappell, C.R., 1972. Recent satellite measurements of the morphology and dynamics of the plasmasphere. Review of Geophysics and Space Physics 10, 951.

Chappell, C.R., 1974. Detached plasma regions in the magnetosphere. Journal of Geophysical Research 79, 1861.

Clauer, C.R., McPherron, R.L., 1974. Mapping the local time—universal time development of magnetospheric substorms using mid-latitude magnetic observations. Journal of Geophysical Research 79, 2811.

Clauer, C.R., McPherron, R.L., 1980. The relative importance of the interplanetary electric field and magnetospheric substorms on partial ring current development. Journal of Geophysical Research 85, 6747.

Clauer, C.R., Liemohn, M.W., Kozyra, J.U., Reno, M.L., 2003. The relationship of storms and substorms determined from mid-latitude ground-based magnetic maps. In: Sharma, S. (Ed.), On the Relationship Between Storms and Substorms, AGU Monogr. Ser. American Geophysical Union, in press.

Daglis, I.A., 2001. Space storms, ting current and space-atmosphere coupling. In: Daglis, I.A. (Ed.), Space Storms and Space Weather Hazards. Kluwer Academic Publishers, Dordrecht, pp. 1–42.

Dasso, S., Gómez, D., Mandrini, C.H., 2002. Ring current decay rates of magnetic storms: a statistical study from 1957 to 1998. Journal of Geophysical Research 107, 10.1029/2000JA000430.

Davis, T.N., Parthasarathy, R., 1967. The relationship between polar magnetic activity *D*p and growth of the geomagnetic ring current. Journal of Geophysical Research 72, 5825.

Dessler, A.J., Parker, E.N., 1959. Hydromagnetic theory of geomagnetic storms. Journal of Geophysical Research 64, 2239.

Ebihara, Y., Ejiri, M., 1998. Modeling of solar wind control of the ring current buildup: a case study of the magnetic storms in April 1997. Geophysical Research Letters 25, 3751–3754.

Ebihara, Y., Ejiri, M., 2000. Simulation study on fundamental properties of the storm-time ring current. Journal of Geophysical Research 105, 15843.

Feldstein, Y.I., Dremukhina, L.A., Mall, U., Woch, J., 2000. On the two-phase decay of the D_{st}-variation. Geophysical Research Letters 27, 2813.

Fok, M.-C., Kozyra, J.U., Nagy, A.F., Rasmussen, C.E., Khazanov, G.V., 1993. Decay of equatorial ring current ions and associated aeronomical consequences. Journal of Geophysical Research 98, 19381.

Frank, L.A., 1970. Direct detection of asymmetric increases of extraterrestrial 'ring current' proton intensities in the outer radiation zone. Journal of Geophysical Research 75, 1263.

Friedel, R.H.W., Korth, H., Henderson, M.G., Thomsen, M.F., Scudder, J.D., 2001. Plasma sheet access to the inner magnetosphere. Journal of Geophysical Research 106, 5845.

Friedrich, E., Rostoker, G., Connors, M.G., 1999. Influence of the substorm current wedge on the D_{st} index. Journal of Geophysical Research 104, 4567–4575.

Fukushima, N., Kamide, Y., 1973. Partial ring current models for worldwide geomagnetic disturbances. Review of Geophysics and Space Physics 11, 795–853.

Ganushkina, N.Yu., Pulkkinen, T.I., Kubyshkina, M.V., Singer, H.J., Russell, C.T., 2002. Modeling the ring current magnetic field during storms. Journal of Geophysical Research 107, 10.1029/2001JA900101.

Gonzalez, W.D., Joselyn, J.A., Kamide, Y., Kroehl, H.W., Rostoker, G., Tsurutani, B.T., Vasyliunas, V.M., 1994. What is a geomagnetic storm? Journal of Geophysical Research 99, 5771.

Grebowsky, J.M., Tulunay, Y., Chen, A.J., 1974. Temporal variations in the dawn and dusk midlatitude trough and plasmapause position. Planetary and Space Science 22, 1089.

Greenspan, M.E., Hamilton, D.C., 2000. A test of the Dessler-Parker-Sckopke relation during magnetic storms. Journal of Geophysical Research 105, 5419.

Hamilton, D.C., Gloeckler, G., Ipavich, F.M., Studemann, W., Wilkey, B., Kremser, G., 1988. Ring current development during the great geomagnetic storm of February 1986. Journal of Geophysical Research 93, 14343.

Jordanova, V.K., Kistler, L.M., Kozyra, J.U., Khazanov, G.V., Nagy, A.F., 1996. Collisional losses of ring current ions. Journal of Geophysical Research 101, 111.

Jordanova, V.K., Farrugia, C.J., Quinn, J.M., Thorne, R.M., Ogilvie, K.W., Lepping, R.P., Lu, G., Lazarus, A.J., Thomsen, M.F., Belian, R.D., 1998. Effects of wave-particle interactions on ring current evolution for January 10–11, 1997: initial results. Geophysical Research Letters 25, 2971.

Jordanova, V.K., Torbert, R.B., Thorne, R.M., Collin, H.L., Roeder, J.L., Foster, J.C., 1999. Ring current activity during the early $Bz < 0$ phase of the January 1997 magnetic cloud. Journal of Geophysical Research 104, 24895–24914.

Jordanova, V.K., Kistler, L.M., Farrugia, C.J., Torbert, R.B., 2001. Effects of inner magnetospheric convection on ring current dynamics: March 10–12, 1998. Journal of Geophysical Research 106, 29705.

Kamide, Y., 2001. Geomagnetic storms as a dominant component of space weather: classic picture and recent issues. In: Daglis, I.A. (Ed.), Space Storms and Space Weather Hazards. Kluwer Academic Publishers, Dordrecht, pp. 43–78.

Kamide, Y., Yokoyama, N., Gonzalez, W., Tsurutani, B.T., Daglis, I.A., Brekke, A., Masuda, S., 1998. Two-step development of geomagnetic storms. Journal of Geophysical Research 103, 6917–6921.

Koch Jr., G.S., Link, R.F., 1980. Statistical Analysis of Geological Data, Vol. 1. Dover, New York.

Korth, H., Thomsen, M.F., Borovsky, J.E., McComas, D.J., 1999. Plasma sheet access to geosynchronous orbit. Journal of Geophysical Research 104, 25047.

Kozyra, J.U., Jordanova, V.K., Borovsky, J.E., Thomsen, M.F., Knipp, D.J., Evans, D.S., McComas, D.J., Cayton, T.E., 1998. Effects of a high-density plasma sheet on ring current development during the November 2–6, 1993 magnetic storm. Journal of Geophysical Research 103, 26285.

Kozyra, J.U., Liemohn, M.W., Clauer, C.R., Ridley, A.J., Thomsen, M. F., Borovsky, J.E., Roeder, J.L., Jordanova, V.K., 2002. Two-step D_{st} development and ring current composition changes during the 4–6 June 1991 magnetic storm. Journal of Geophysical Research 1224, doi: 10.1029/2001JA000023.

Liemohn, M.W., Kozyra, J.U., Jordanova, V.K., Khazanov, G.V., Thomsen, M.F., Cayton, T.E., 1999. Analysis of early phase ring current recovery mechanisms during geomagnetic storms. Geophysical Research Letters 25, 2845–2848.

Liemohn, M.W., 2003. Yet another caveat to using the Dessler–Parker–Sckopke relation. Journal of Geophysical Research, in press.

Liemohn, M.W., Kozyra, J.U., Thomsen, M.F., Roeder, J.L., Lu, G., Borovsky, J.E., Cayton, T.E., 2001a. Dominant role of the

asymmetric ring current in producing the stormtime D_{st}^{*}. Journal of Geophysical Research 106, 10883.

Liemohn, M.W., Kozyra, J.U., Clauer, C.R., Ridley, A.J., 2001b. Computational analysis of the near-Earth magnetospheric current system. Journal of Geophysical Research 106, 29531.

Liemohn, M.W., Kozyra, J.U., Clauer, C.R., Khazanov, G.V., Thomsen, M.F., 2002. Adiabatic energization in the ring current and its relation to other source and loss terms. Journal of Geophysical Research 107, 1045. doi: 10.1029/2001JA000243.

Lindsay, G.M., Russell, C.T., Luhmann, J.G., 1999. Predictability of D_{st} index based upon solar wind conditions monitored inside. Journal of Geophysical Research 104, 10335.

Lui, A.T.Y., McEntire, R.W., Krimigis, S.M., 1987. Evolution of the ring current during two geomagnetic storms. Journal of Geophysical Research 92, 7459–7970.

Maguire, J.J., Carovillano, R.L., 1968. Effect of the interplanetary field on energy of geomagnetic disturbances. Journal of Geophysical Research 73, 3395.

Maltsev, Y.P., Ostapenko, A.A., 2002. Comment on "Evaluation of the tail current contribution to D_{st}" by N.E. Turner, et al. Journal of Geophysical Research 107, 10.1029/2001JA000098.

Maynard, N.C., Chen, A.J., 1975. Isolated cold plasma regions: Observations and their relation to possible production mechanisms. Journal of Geophysical Research 80, 1009.

McIlwain, C.E., 1986. A *K*p dependent equatorial electric field model. Advances in Space Research 6 (3), 187.

Mitchell, D.G., Hsieh, K.C., Curtis, C.C., Hamilton, D.C., Voss, H.D., Roelof, E.C., C:son Brandt, P., 2001. Imaging two geomagnetic storms in energetic neutral atoms. Geophysical Research Letters 28, 1151.

Munsami, V., 2000. Determination of the effects of substorms on the storm-time ring current using neural networks. Journal of Geophysical Research 105, 27,833.

O'Brien, T.P., McPherron, R.L., 2000a. An empirical phase space analysis of ring current dynamics: solar wind control of injection and decay. Journal of Geophysical Research 105, 7707–7719.

O'Brien, T.P., McPherron, R.L., 2000b. Forecasting the ring current index D_{st} in real time. Journal of Atmospheric and Solar-Terrestrial Physics 62, 1259.

Ohtani, S., Nosé, M., Rostoker, G., Singer, H., Lui, A.T.Y., Nakamura, M., 2001. Storm-substorm relationship: contribution of the tail current to D_{st}. Journal of Geophysical Research 106, 21199.

Pollock, C.J., et al., 2001. Initial Medium Energy Neutral Atom (MENA) images of Earth's magnetosphere during substorms and stormtime. Geophysical Research Letters 28, 1147.

Rairden, R.L., Frank, L.A., Craven, J.D., 1986. Geocoronal imaging with dynamics explorer. Journal of Geophysical Research 91, 13613.

Richmond, A.D., Kamide, Y., 1988. Mapping electrodynamic features of the high-latitude ionosphere from localized observations: technique. Journal of Geophysical Research 93, 5741.

Roeder, J.L., Fennell, J.F., Chen, M.W., Grande, M., Livi, S., Schulz, M., 1996. CRRES observations of stormtime ring current ion composition. In: Reeves, G.D. (Ed.), Workshop on the Earth's Trapped Particle Environment, AIP Conference Proceedings, Vol. 383. American Institute of Physics, New York, pp. 131–143.

Rostoker, G., 1972. Geomagnetic indices. Review of Geophysics and Space Physics 10, 935–950.

Rostoker, G., 2000. Effects of substorms on the stormtime ring current index D_{st}. Annals of Geophysics 18, 1390.

Sckopke, N., 1966. A general relation between the energy of trapped particles and the disturbance field near the Earth. Journal of Geophysical Research 71, 3125.

Shen, C., Liu, Z., Kamei, T., 2002. A physics-based study of the D_{st}-AL relationship. Journal of Geophysical Research 107, 10.1029/2001JA900121.

Takahashi, S., Iyemori, T., Takeda, M., 1990. A simulation of the storm-time ring current. Planetary and Space Science 38, 1133–1141.

Temerin, M., Li, X., 2002. A new model for the prediction of dst on the basis of the solar wind. Journal of Geophysical Research in press.

Tsyganenko, N., Stern, D.P., 1996. Modeling the global magnetic field of the large-scale Birkeland current systems. Journal of Geophysical Research 101, 27187–27198.

Tsyganenko, N.A., 2000a. Solar wind control of the tail lobe magnetic field as deduced from Geotail, AMPTE/IRM, and ISEE 2 data. Journal of Geophysical Research 105, 5517–5528.

Tsyganenko, N.A., 2000b. Modeling the inner magnetosphere: The asymmetric ring current and Region 2 Birkeland currents revisited. Journal of Geophysical Research 105, 27739–27754.

Turner, N.E., Baker, D.N., Pulkkinen, T.I., McPherron, R.L., 2000. Evaluation of the tail current contribution to D_{st}. Journal of Geophysical Research 105, 5431.

Turner, N.E., Baker, D.N., Pulkinnen, T.I., Roeder, J.L., Fennell, J.F., Jordanova, V.K., 2001. Energy content in the stormtime ring current. Journal of Geophysical Research 106, 19149.

Turner, N.E., Baker, D.N., Pulkkinen, T.I., McPherron, R.L., 2002. Reply. Journal of Geophysical Research 107, 10.1029/2001JA900099.

Waters, C.L., Anderson, B.J., Liou, K., 2001. Estimation of global field aligned currents using the iridium system magnetometer data. Geophysical Research Letters 28, 2165.